Visualization of membrane localization and functional state of CB_2R pools by matched agonist and inverse agonist probe pairs

M. Wasinka-Kalwa,[a] ¥ A. Omran,[a] ¥ L. Mach,[a] J. Bouma,[b] L. Scipioni,[c] X. Li,[d,e] S. Radetzki,[a] Y. Mostinski,[a] M. Schippers,[f] T. Gazzi,[a], C. van der Horst,[b] B. Brennecke,[a] A. Hanske,[a] Y. Kolomeets,[a] W. Guba,[f] D. Sykes,[g,h], J. P. von Kries,[a] J. Broichhagen,[a] T. Hua,[d,e] D. Veprintsev,[g,h] L. H. Heitman,[b] S. Oddi,[i] M. Maccarrone,[c] U. Grether[f]* and M. Nazare[a]*

[a] *Leibniz-Forschungsinstitut für Molekulare Pharmakologie FMP, Campus Berlin-Buch, 13125 Berlin (Germany), E-mail: nazare@fmp-berlin.de*

[b] *Division of Drug Discovery and Safety, Leiden Academic Centre for Drug Research, Leiden University, 2333 CC, Leiden (The Netherlands)*

[c] *Department of Biotechnological and Applied Clinical Sciences, University of L'Aquila, Via Vetoio snc, 67100 L'Aquila & Lipid Neurochemistry Unity - CERC at IRCCS Santa Lucia Foundation, 00164 Rome (Italy)*

[d] *iHuman Institute, ShanghaiTech University, Shanghai 201210, China*

[e] *School of Life Science and Technology, ShanghaiTech University, Shanghai 201210, China*

[f] *Roche Pharma Research & Early Development, Roche Innovation Center Basel, F. Hoffmann-La Roche Ltd., 4070 Basel (Switzerland), E-mail: uwe.grether@roche.com*

[g] *Division of Physiology, Pharmacology & Neuroscience, School of Life Sciences, University of Nottingham, Nottingham, NG7 2UH, UK*

[h] *Centre of Membrane Proteins and Receptors (COMPARE), University of Birmingham and University of Nottingham, Midlands, UK*

[i] *Department of Veterinary Medicine, University of Teramo, Via R. Balzarini 1, 64100 Teramo (Italy) & Lipid Neurochemistry Unity - CERC at IRCCS Santa Lucia Foundation, 00164 Rome (Italy)*

Abstract

The diversity of physiological roles of the endocannabinoid system has turned it into an attractive yet elusive therapeutic target. However, chemical probes with various functionalities could pave the way for a better understanding of the endocannabinoid system at the cellular level. Notably, inverse agonists of CB_2R – a key receptor of the endocannabinoid system - lagged behind despite the evidence regarding the therapeutic potential of its antagonism. Herein, we report a matched fluorescent probe pair based on a common chemotype to address and visualize both the active and inactive states of CB_2R, selectively. Alongside with extensive cross-validation by flow cytometry and confocal microscopy, we successfully visualize the intracellular localization of CB_2R pools in live cells. The synthetic simplicity together with the high CB_2R-selectivity and specificity of our probes, turn them into valuable tools in chemical biology and drug development that can benefit the clinical translatability of CB_2R-based drug.

https://doi.org/10.26434/chemrxiv-2024-q741f **ORCID:** https://orcid.org/0000-0002-1602-2330 Content not peer-reviewed by ChemRxiv. **License:** CC BY-NC-ND 4.0

Introduction

The endocannabinoid system (ECS) is a complex lipid-based signalling network involved in a wide variety of physiological and cognitive processes such as pain regulation, immune response, appetite control, learning and memory formation, cardiovascular regulation, and addictive-like behaviour.[1] The ECS consists of two cannabinoid receptor subtypes (CB_1R and CB_2R) that belong to the class A G protein-coupled receptor (GPCR) family. Arachidonoylethanolamide (AEA) and 2-arachidonoylglycerol (2-AG) are the endogenous ligands of both CB_1R and CB_2R.[2] Regardless of their high homology, the key difference between the two receptors is their distribution.[3] CB_1R is predominantly expressed in the central nervous system with the highest density in cerebellum, hippocampus, and cerebral cortex,[4-6] while CB_2R is more abundant in peripheral organs such as spleen and tonsils, and is mainly expressed in cells associated with the immune system.[3] It has been shown that expression of CB_2R is strongly upregulated in pathological conditions such as cancer,[7, 8] immunological disorders,[9] inflammation, neurodegenerative diseases,[10, 11] and drug abuse.[12] Therefore, modulating CB_2R activation will be a valuable therapeutic approach for several diseases including inflammation, autoimmune and metabolic disorders, chronic pain, multiple sclerosis and cancer. For example, agonist-mediated activation of CB_2R was previously shown to be beneficial for neuroprotection in chronic neurodegenerative disorders such as Huntington's and Alzheimer's diseases.[13] Conversely, inactivation of CB_2R via an inverse agonist/antagonist was found to have therapeutic potential for treatment of various diseases associated with neuroinflammation and immune system.[14, 15] Due to different expression patterns of CB_2R and CB_1R, as well as to their distinct functions, the selective activation or deactivation of CB_2R does not involve undesired psychotropic responses which has been granted a great therapeutic advantage over CB_1R. However, despite its great potential, no CB_2R-selective drug has made its way to market to date, as clinical translatability from preclinical models deduced from different species is currently challenging.[14] This is largely attributed to highly inducible nature and complexity of CB_2R signalling pathways at the cellular level and the unclear understanding of its expression, localization and function.[16] For example, a number of studies indicate that the cellular responses associated with CB_2R activation are not only limited to plasmalemmal receptors but also to the intracellular pools.[17-19] The absence of CB_2R-specific monoclonal antibodies, which are important tools for obtaining expression data at a cellular or tissue level, is further aggravating this situation.

While recent CB_2R-selective agonist fluorescent probes[20-22] could partially fill these gaps by addressing the activated state and providing information on CB_2R localization, expression, target engagement, pharmacokinetic and dynamics in real-time; the scarcity of labeled CB_2R-selective inverse agonist

https://doi.org/10.26434/chemrxiv-2024-q741f **ORCID:** https://orcid.org/0000-0002-1602-2330 Content not peer-reviewed by ChemRxiv. **License:** CC BY-NC-ND 4.0

probes has resulted in a lack of information on the distribution of intra- and extracellular CB_2R pools in the inactivated state. There are only a limited number of reports about inverse agonist fluorescent probes labeling CB_2R. For example, the chromenopyrazole-based inverse agonist probe was originally generated from an agonist but upon attachment of the Cy5 fluorescent dye, the functionality was altered.[23] The surface receptors of CB_2R expressing HEK-293 cells were labeled via the aforementioned probe.[23] Another example is **NIR-mbc94**, an analogue of selective inverse agonist **SR144528**, which has been shown to be an imaging agent for the unbiased high-throughput screening of compounds interacting with CB_2R as therapeutic target.[24] Despite the wide range of applications and a high demand for CB_2R inverse agonist probes, no versatile probe platform with diverse fluorophores is available so far.

We have previously reported on a high-affinity, cell-permeable fluorescent CB_2R probe **3** based on a reverse-design approach using a preclinically validated drug-derived CB_2R agonist **1** (Figure 1 and Figure 2).[20] The probe successfully detected CB_2R in several *in vitro* and *in vivo* settings across species. For example, **3** was also recently used to visualize the high expression levels of CB_2R in primary neonatal microglia isolated from wild-type and Tg2576 mice, the latter is used as an Alzheimer's Disease (AD) model.[25]

However, for any chemical probe approach, it is desirable to have access to a matched molecular pair of agonist and inverse agonist with high structural similarity which are correspondingly labeled. Such chemical probes are most suitable to address distinct mechanisms of actions, e.g. by distinguishing the activated or resting state of the receptor or allowing differential analysis of agonist-stimulated internalization of the receptor, while excluding the cellular phenotype.

With the goal of expanding the scope of our probe platform and addressing both active and inactive states of the receptor, we designed a matched molecular pair of CB_2R agonist and antagonist fluorescent probes derived from highly similar chemotypes of advanced preclinical CB_2R agonist **1** and inverse agonist **2** drug candidates (Figure 1). In addition, we were able to attach a variety of fluorescent dyes leading to CB_2R probes that span a broad range of physicochemical properties. At last, varying combinations of agonist and antagonist with cell-permeable (e.g. TAMRA) or impermeable (e.g. Alexa488) fluorophores gave us access to a valuable tool box suitable for detecting extra- and intracellular receptor pools. To explore the spatial-temporal dynamics of CB_2R, we employed these novel probes to investigate the expression and subcellular localization of the active and inactive states of the CB_2R in living cells, utilizing super-resolution confocal imaging techniques.

https://doi.org/10.26434/chemrxiv-2024-q741f **ORCID:** https://orcid.org/0000-0002-1602-2330 Content not peer-reviewed by ChemRxiv. **License:** CC BY-NC-ND 4.0

Results and discussion

Probe design and molecular modelling

Our previous probes were derived from a drug-like CB_2R agonist bearing a 5,6-substituted picolinamide **1** (Figure 1). Interestingly, it was shown that different substitutions at the 5- and 6-position of picolinamide could alter the functionality of the ligand while maintaining high CB_2R affinity.[26, 27] For example, the replacement of cyclopropyl moiety at position 5 of agonist **1** by a 3-methoxy-azetidine alters the functionality from agonism to inverse agonism (**2**). This substitution causes a flip of the side chain of the toggle switch residue W258$^{6.48}$ (Ballesteros-Weinstein numbering in superscript, Figure 2B).[28] Besides the 5,6-substitutents, both ethyl side chains are involved in favorable van der Waals interactions with surrounding phenylalanine side chains F91, F94, F106.

The drug-derived inverse agonist **2** possessing an exceptional selectivity profile (CB_2R K_i = 0.3 nM; CB_1R K_i = 721 nM; selectivity factor of 2,403 over CB_1R) was an ideal starting point for generating a matched agonist and inverse agonist-based probe pair with a 5,6-substituted picolinamide core in common.[26, 29, 30]

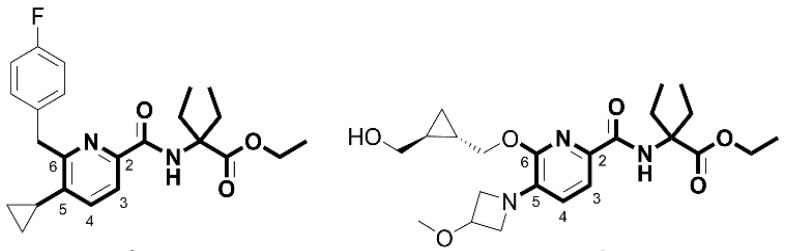

Figure 1. Chemical structures of CB_2R agonist **1** and inverse agonist **2** sharing 5- and 6-substituted picolinamide core.

The first and the most critical step in probe design is the identification of a suitable attachment point between the recognition element and the reporter unit, i.e. ligand and fluorescent dye, respectively. In most cases, the recognition element and the fluorescent dye are distanced using a suitable linker, which allows the dye to access to extracellular space without compromising overall binding affinity.[31] Previously, we have introduced a hybrid of thio- and polyether chain to one of the ethyl groups of the diethylglycine moiety as the centerpiece hub (**3**, Figure 2A). Even though our previous probes showed highly consistent interspecies affinity and potency for both human and mouse CB_2R, the presence of the sulfur atom in the linker posed a possible experimental imponderability in some of the advanced settings, as sulfur might be prone to oxidation.[20, 32] Therefore, with the goal of improving the physicochemical properties and simplifying the synthetic strategy, SAR studies were performed to

https://doi.org/10.26434/chemrxiv-2024-q741f **ORCID:** https://orcid.org/0000-0002-1602-2330 Content not peer-reviewed by ChemRxiv. **License:** CC BY-NC-ND 4.0

investigate alternative sites for linker attachment at the diethylglycine centerpiece hub. For this we used the ester functionality which after substitution by an amide moiety served as attachment point. This design approach has the advantage that no chiral center is present and the synthesis route is greatly simplified compared to our previous probes (**4**, Figure 2A).

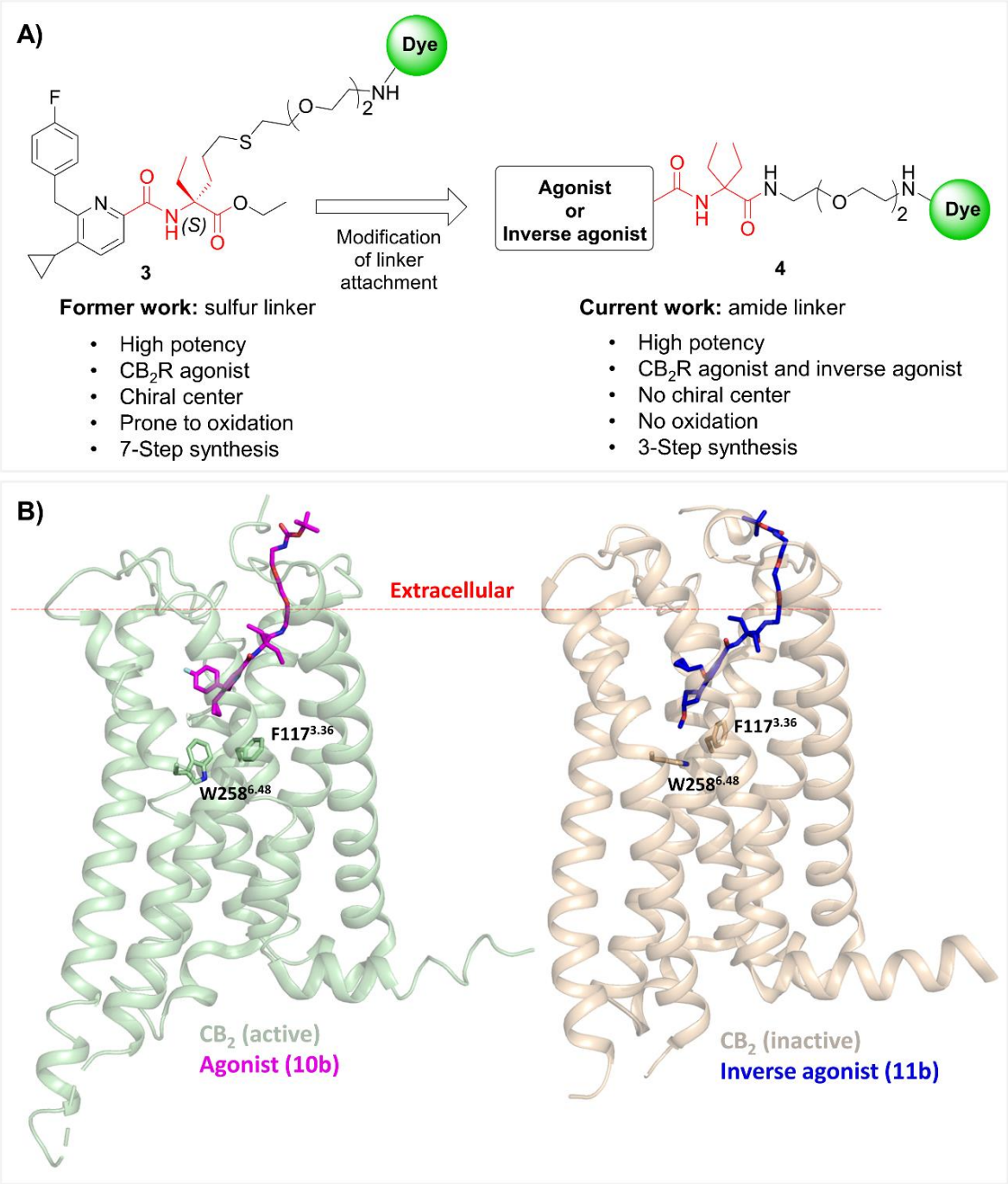

Figure 2. A) Modification of linker attachment from previous work (compound **3**; sulfur linker) led to the discovery of a new versatile exit vector (compound **4**; amide linker), diethylglycine moiety as centerpiece hub in red. B) Docking poses of compounds **10b** (magenta sticks) and **11b** (blue sticks) within active (green; PDB: 6KPF) and inactive (orange; PDB: 5ZTY) states of CB_2R, respectively. Red dashed line indicates the approximate boundary of the lipid bilayers. For detailed description of the docking studies see SI, S3.

https://doi.org/10.26434/chemrxiv-2024-q741f **ORCID:** https://orcid.org/0000-0002-1602-2330 Content not peer-reviewed by ChemRxiv. **License:** CC BY-NC-ND 4.0

Docking experiments were conducted to estimate the required linker length to reach out into the extracellular space and support linkerology studies. In Figure 2B the best docking poses for agonist (**10b**) and inverse agonist (**11b**) pharmacophores, respectively, are depicted. For both ligands, the proper range of PEG chains to access to the extracellular space for insertion of the fluorescent dye was estimated to be n=2.

Chemistry

The synthetic pathway to access the Boc-protected intermediates and target fluorescent probes bearing various dyes is outlined in Scheme 1. Fmoc-protected diethylglycine **5** was used as the centerpiece unit to connect the 5,6-substituted picolinamide recognition elements to the desired linker. In order to elaborate the optimal linker length for dye attachment, compound **5** was functionalized with a series of linkers **6a-d** with different lengths under HATU-mediated amide coupling conditions. Fmoc-protecting group removal of compounds **7a-d** using DBU was followed by coupling to agonist **8** or inverse agonist **9** precursors *in situ* to afford Boc-protected congeners with matched chemotypes (**10a-d** and **11a-d**). Compounds **8**[20] and **9**[30] were synthesized according to literature protocols. The final step was to conjugate a variety of broadly used fluorophores such as 5/6-TAMRA, SiR, 5/6-Alexa488 and Alexa647 to the selected intermediates (**10b** and **11b**) with the linker length of n=2, which turned out to be optimal in subsequent SAR studies. For this purpose, the Boc-protecting group of **10b** or **11b** was first cleaved using TFA. Subsequently, the resulting free amines were coupled with the desired fluorescent dyes either under suitable amide coupling or nucleophilic aromatic substitution conditions to furnish probes **12-15** and **17-18**. Compound **16** was synthesized via a variation of the aforementioned synthetic route starting with coupling of 5/6-TAMRA-COOH to Boc-deprotected **7b** followed by another amide coupling reaction to **9** using HATU as coupling reagent (Suppl. Information, S32).

https://doi.org/10.26434/chemrxiv-2024-q741f **ORCID:** https://orcid.org/0000-0002-1602-2330 Content not peer-reviewed by ChemRxiv. **License:** CC BY-NC-ND 4.0

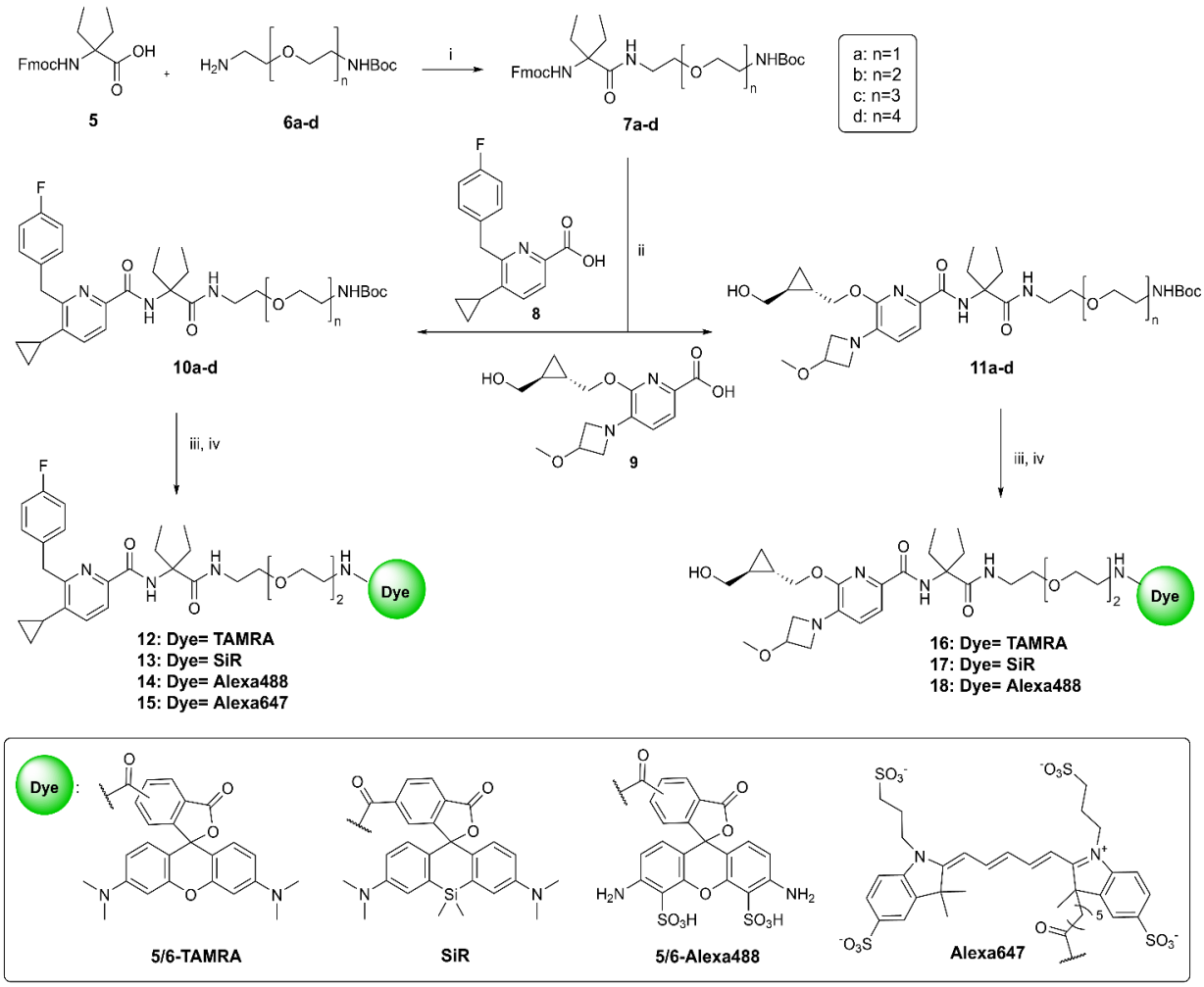

Scheme 1. Synthesis of fluorescent probes. Reagents and conditions: i) HATU, DIPEA, DMF, rt, 1h. ii) (1) DBU, HOAt, DMF, rt, 20 min; (2) **8** or **9**, HATU, DIPEA, DMF, rt, 10h; iii) TFA (9 equiv.), CH_2Cl_2, 0 °C to rt, 3h; iv) for compounds **13**, **15**, **17** and **18**: HATU, dye, DIPEA, DMF, rt, 10h; for compound **12**: EDC·HCl, HOAT, dye, DIPEA, DMF, rt, 10h; for compound **14**: dye, DIPEA, DMF, rt, 10h; for compound **16**: see the suppl. information.

Evaluation of the appropriate linker length

To identify the optimal linker length, binding affinities of unlabeled precursors **10a-d** and **11a-d** were measured via a competitive radioligand binding assay on CHO membranes stably expressing hCB_1R or hCB_2R (Table 1).

For both agonist and inverse agonist chemotypes, the PEG chain with n=2 (**10b** and **11b**, respectively) showed the highest affinity and selectivity for CB_2R, and was therefore chosen as the optimal linker length. This selection was also supported by our docking studies (Figure 2B). To assess whether the attachment of the linker affects receptor function, the efficacy of selected precursors was determined in a cAMP assay (Table 1). To our delight, **10b** and **11b** preserved partial agonist and inverse agonist activity, respectively, with high potency (CB_2R cAMP EC_{50}=49 nM for **10b** and IC_{50}=88 nM for **11b**, respectively).

https://doi.org/10.26434/chemrxiv-2024-q741f **ORCID:** https://orcid.org/0000-0002-1602-2330 Content not peer-reviewed by ChemRxiv. **License:** CC BY-NC-ND 4.0

Table 1. Binding affinities and potency of the Boc-protected intermediates

Cmpd	Linker length	K_i [a] (nM)		Selectivity [b]	EC_{50} or IC_{50} [c] (nM)	E_{max} (%) [d]	Function
		hCB_1R	hCB_2R				
10a	n=1	836	28	30	n.d.	n.d.	n.d.
10b	n=2	466	6	78	49	83	agonist
10c	n=3	748	63	12	n.d.	n.d.	n.d.
10d	n=4	1,472	144	10	n.d.	n.d.	n.d.
11a	n=1	>10,000	2,061	>4	n.d.	n.d.	n.d.
11b	n=2	>10,000	106	>94	88	-63	inverse agonist
11c	n=3	>10,000	>10,000	n.a.	n.d.	n.d.	n.d.

[a] K_i (nM) values obtained from [^{3}H]CP55,940 displacement assays on CHO membranes stably expressing hCB_1R or hCB_2R. Values are means of at least three independent experiments performed in duplicate. For details, see Suppl. Information. [b] Selectivity was determined by calculating the ratio of K_i (CB_1R)/K_i (CB_2R). [c] The potency (EC_{50} or IC_{50}) of the selected compounds were measured using cells stably expressing hCB_2R in homogeneous time-resolved fluorescence (HTRF®) cAMP assay. The data are the means of four independent experiments performed in technical replicates. [d] Maximum effect (E_{max} in %) was normalized to reference full agonist **APD371**. n.a. is not applicable. n.d. is not determined.

Pharmacological characterization of fluorescent probes 12-18

Compared to their unlabeled congeners, the binding affinity of the fluorescent probes **12-18** indicated fluorescent dye dependency which is not unexpected as the structural nature of the fluorophore alters the membrane interactions of the constructs. However, most of the probes showed high affinity and selectivity for CB_2R (Suppl. Information, table S- 2).

In functional studies (Table 2), probes **13** and **15** indicated full agonism with potencies (EC_{50}) of approximately 525 nM, while **12** and **14** showed partial agonism with higher potencies (EC_{50}) of approximately 80 nM. As anticipated, the functional mode of action of probes **16-18** fully retained their inverse agonism with IC_{50} values in the range of 114-262 nM (Table 2 and Figure 3).

To assess the specificity of the probes and scout for putative off-targets, TAMRA-probe pairs **12** and **16** were screened against a customized panel of 50 representative receptors and enzymes.[33] Both probes were devoid of any relevant off-target interactions thus confirming their suitability for specific CB_2R detection studies (Suppl. Information, table S- 1).

For high probe quality a lower lipophilicity is crucial as it significantly reduces non-specific binding.[34] Therefore, it is noteworthy that all predicted clogD values of our drug-derived probes showed an overall significantly lower lipophilicity range compared to phytocannabinoids[21] and are in a favorable drug-like range (Table 2). Moreover, except for highly ionized sulfonated fluorescent dyes such as Alexa488 and Alexa647 (**14**, **15** and **18**), attachment of TAMRA (**12** and **16**) and SiR (**13** and **17**) did not lead to a significant change in the lipophilicity of the final probes compared to their unlabeled counterparts (**10b** $clogD_{7.4}$=3.796 and **11b** $clogD_{7.4}$=3.194).

https://doi.org/10.26434/chemrxiv-2024-q741f **ORCID:** https://orcid.org/0000-0002-1602-2330 Content not peer-reviewed by ChemRxiv. **License:** CC BY-NC-ND 4.0

Table 2. hCB_2R potency and predicted $logD_{7.4}$ of fluorescent probes **12-18**

Cmpd	EC_{50} or IC_{50} (nM) [a]	E_{max} (%) [b]	Function	$clogD_{7.4}$ [c]
12	82	80	partial agonist	3.662
13	528	127	full agonist	3.868
14	77	79	partial agonist	-0.495
15	523	129	full agonist	-0.881
16	114	-29	inverse agonist	3.633
17	129	-29	inverse agonist	2.234
18	262	-26	inverse agonist	-0.915

[a] The potency (EC_{50} or IC_{50}) of fluorescent probes **12-18** were measured using cells stably expressing hCB_2R in homogeneous time-resolved fluorescence (HTRF®) cAMP assay. The data are the means of four or seven independent experiments performed in technical replicates. [b] Maximum effect (E_{max} in %) was normalized to reference full agonist **APD371**.[c] For computational calculation of $clogD_{7.4}$ see reference.[35]

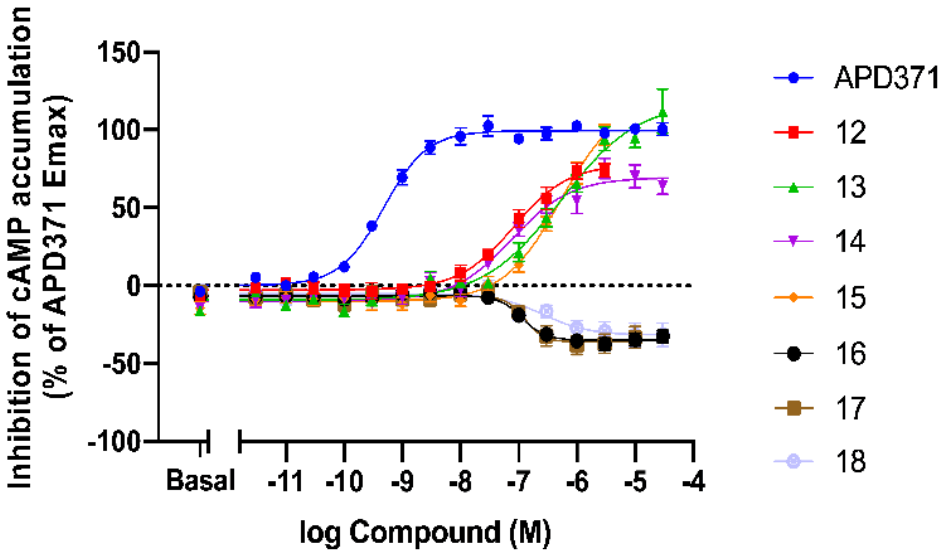

Figure 3. Inhibition of cAMP accumulation on hCB_2R were determined with a (HTRF®) cAMP assay. Maximum effect (E_{max} in %) was normalized to reference full agonist **APD371**.

https://doi.org/10.26434/chemrxiv-2024-q741f **ORCID:** https://orcid.org/0000-0002-1602-2330 Content not peer-reviewed by ChemRxiv. **License:** CC BY-NC-ND 4.0

Cellular imaging by flow cytometry and confocal microscopy in live cells

The probe's specificity and suitability for imaging were further validated by flow cytometry. All the fluorescent probes were incubated with various concentrations ranging from 0.014 to 10 µM in live CHO cells overexpressing hCB_1R or hCB_2R and wild-type (wt) CHO cells as control. Despite some differences observed in the mean fluorescence intensity (MFI) of probes bearing the same dyes, most of the tested probes indicated decent selectivity and specificity for hCB_2R in flow cytometry, suggesting their suitability for imaging applications (Suppl. Information, figure S-1). To exclude unspecific binding, we further examined the effect of preincubation of cells with high-affinity competitor ligands such as agonist **JWH133**[36] and inverse agonist **RO6851228**[37] on probe **15** binding (Suppl. Information, figure S-2). Both ligands competed with **15** in a dose-dependent manner confirming high target specificity of **15** for CB_2R.

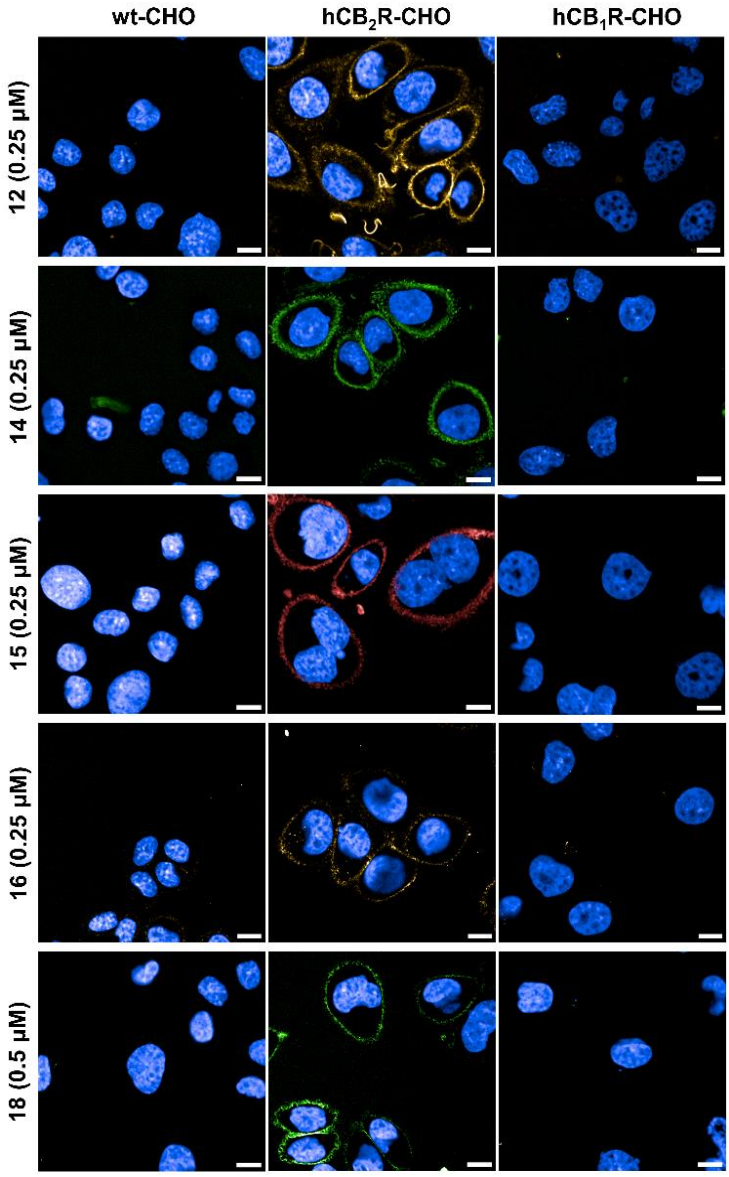

Figure 4. Kinetic confocal microscopy in live cells. The wild type (wt) and overexpressing hCB_2R and hCB_1R CHO cells were co-stained with probes **12**, **14-16** and **18** and Hoechst 33342 (blue, nucleus counter stain). The images were recorded 10 min after probe incubation. Images are representative of two independent experiments. Scale bars, 10 µm.

https://doi.org/10.26434/chemrxiv-2024-q741f **ORCID:** https://orcid.org/0000-0002-1602-2330 Content not peer-reviewed by ChemRxiv. **License:** CC BY-NC-ND 4.0

Based on the high specificity of our probes we continued our investigation by performing kinetic confocal microscopy experiments to visualize hCB_2R in live CHO cells. For selected probes, blocking experiments with competitive non-labeled ligands **RO6851228**[37] (CB_2R-inverse agonist) and/or **RO6871304**[38] (CB_2R-agonist) were carried out as well (Suppl. Information, figure S-3). Figure 4 displays the frames of CHO cells overexpressing hCB_2R and hCB_1R along with parental CHO cells 10 min after administration of probes **12**, **14-16** and **18**. All probes, selectively stained the CB_2R on the cell membrane.

Super-resolution confocal imaging of hCB_2-CHO cells

Next, by using super-resolution confocal imaging, we assessed the intensity and subcellular distribution of fluorescence staining produced by the matched TAMRA-probe pair **12** and **16** on hCB_2R overexpressing CHO cells. Image acquisition at higher magnification and resolution was performed after 15 minutes of incubation with **12** and **16**, revealed that both probes yielded a similar localization pattern, yet with very distinct labeling intensity. Indeed, for both probes the CB_2R staining was primarily observed intracellularly, especially in the perinuclear membranes that are suggestive of the Golgi apparatus and the endoplasmic reticulum; however, an appreciable intracellular fluorescence was also present on the cell membrane (Figure 5A and B). Notably, these results corroborate and extend the findings previously reported by den Boon et al.[18]

It is noteworthy that the analysis of MFI of **12**-labeled CB_2R showed a plasma membrane labeling intensity of the CB_2R approximately six-fold higher than that of **16**-labeled CB_2R (**12**-labeled CB_2R = 2090 ± 175 MFI; **16**-labeled CB_2R = 350 ± 4 MFI; unpaired *t*-test, t = 19.94, df = 4, p-value < 0.0001). Similarly, when examining the intracellular compartments, a marked difference in MFI values was observed (**12**-labeled CB_2R = 2575 ± 100 MFI; **16**-labeled CB_2R = 340 ± 13 MFI; unpaired *t*-test, t = 37.57, df = 4, p-value < 0.0001). This marked difference in labeling intensity still persisted even when differences in binding affinities were compensated by increasing the concentration of **16** versus **12** (Suppl. Information, figure S- 4). Moreover, comparable quantum yields of probes **12** and **16** in lipophilic media (Suppl. Information, table S- 4) ruled out a potential interference with the observed differences in MFI.

Given that probes **12** and **16** are conjugated with the identical fluorophore and exhibit comparable physicochemical features, including their binding affinity for the active and inactive form of CB_2R, respectively, (Suppl. Information, table S- 2) the more pronounced signal detected with probe **12** relative to probe **16** indicates that under steady-state conditions in living cells, CB_2R is present predominantly in its active conformation. It is also plausible that the inactive form of the receptor is less accessible for interaction with probe **16** resulting in weaker labeling when compared to probe **12**.[39, 40] Further investigation into the molecular basis of these differences might provide valuable

https://doi.org/10.26434/chemrxiv-2024-q741f **ORCID:** https://orcid.org/0000-0002-1602-2330 Content not peer-reviewed by ChemRxiv. **License:** CC BY-NC-ND 4.0

insights into the interaction dynamics between CB_2R and its ligands, potentially informing the design of more effective probes or therapeutic agents targeting this receptor.

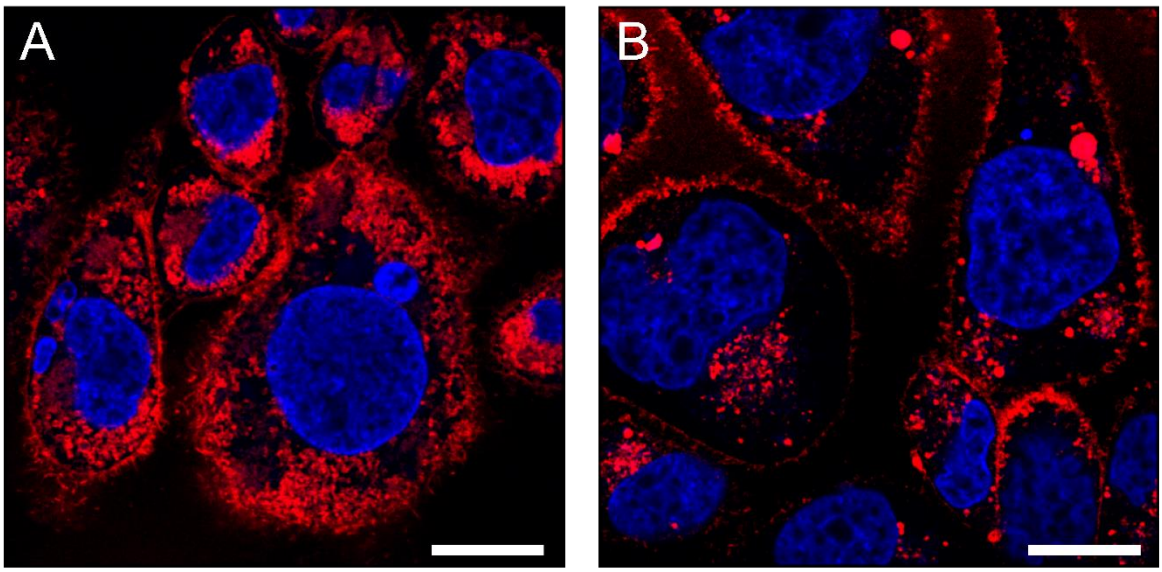

Figure 5. Super-resolution confocal imaging of overexpressing hCB_2 CHO cells. hCB_2R. The cells were stained for 15 min with (A) **12** (0.8 µM, red) or (B) **16** (0.8 µM, red) and Hoechst 33342 (blue, nucleus counter stain). Cells were optically sectioned using confocal laser-scanning microscopy equipped with an Airyscan detector. For quantifying the relative levels of labeling by the two TAMRA-probes, identical imaging settings (*i.e.*, objective, light path, laser power, gain, offset, frame size, zoom and scan speed) were maintained throughout the acquisition process. Images are representative of three independent experiments. Scale bars, 10 µm.

Conclusions

In this study, we have developed the first general CB_2R selective matched agonist or inverse agonist platform using validated drug-derived CB_2R ligands **1** and **2**, respectively, as starting points. We designed fluorescent probes sharing highly similar drug-derived chemotypes but addressing either the active or inactive state of CB_2R. Due to our reverse-design approach using highly drug-like precursors, all labeled probes exhibited favorable physicochemical properties. The key for receptor recognition element and fluorophore attachment was a common centrepiece that allowed simple linker attachment by amide coupling. The probes retained good binding affinity towards CB_2R and high selectivity against CB_1R upon conjugation of fluorescent dyes. When investigating the functional responses in a cellular cAMP accumulation assay, the labeled probes were able to evoke a similar functional response as their unlabeled congeners. In particular, the labeled inverse agonist enabled us to address the resting state of CB_2R. This is of great benefit and importance for various control experiments in live cells which are now possible. Finally, our probes allowed the assessment of localization and distribution of the active and inactive conformations of CB_2R through high-resolution confocal microscopy analysis. These studies indicate that within living cells, a considerable number of

https://doi.org/10.26434/chemrxiv-2024-q741f **ORCID:** https://orcid.org/0000-0002-1602-2330 Content not peer-reviewed by ChemRxiv. **License:** CC BY-NC-ND 4.0

CB_2Rs are located intracellularly and are in an active state. The differential content of the active and inactive states of CB_2R suggests a complex regulatory mechanism governing its activity and interactions with intracellular signalling pathways. These observations have significant implications for understanding the receptor's role in physiological and pathological processes. Furthermore, our approach demonstrates the potential for super-resolution imaging of our CB_2R probes in studying membrane receptors and thus representing a powerful tool for future research in cellular biology and pharmacology.

Author Contributions

M.N., U.G. conceived the research and acquired funding for this project. M.W-K., A.O., L.M., Y.M., T.G., B.B., W.G., D.V., L.H.H., S.O., M.Ma., U.G., M.N. designed the research approach. M.W-K., A.O., L.M., J.B., L.S., X.L., S.R., Y.M., M.S., T.G., C.v.d.H., B.B., A.H., Y.K., W.G., D.S., J.P.v.K., J.Br., T.H., D.V., S.O. performed experiments, analyzed raw data, and worked on probe validation. M.W-K., A.O., L.M., S.O., M.Ma., U.G., M.N. analyzed all data generated, and wrote the manuscript. J.B., Y.M., W.G., J.Br., T.H., D.V., L.H.H. provided useful comments and feedback for the manuscript. All authors have given approval to the final version of the manuscript.

Conflicts of interest

The authors declare no competing financial interest.

Acknowledgements

The authors are grateful to Marta Diceglie, Peter Lindemann, Edgar Specker, Katy Franke, Ramona Birke, Andreas Oder, Astrid Mühl, Peter Schmieder (all Leibniz-Forschungsinstitut für Molekulare Pharmakologie (FMP)), Isabelle Kaufmann, Christian Bartelmus, Oliver Scheidegger, Claudia Korn (all Roche) for their excellent support in sample handling, analytical compound characterization and helpful discussions. This research was partly funded by the the European Union - Next Generation EU - NRRP M6C2 - Investment 2.1 Enhancement and strengthening of biomedical research in the NHS (project No. PNRR-MAD-2022-12376730) to SO and MM.

References

1. D. Friedman, J. A. French and M. Maccarrone, Safety, efficacy, and mechanisms of action of cannabinoids in neurological disorders, *Lancet Neurol.*, 2019, **18**, 504.

https://doi.org/10.26434/chemrxiv-2024-q741f **ORCID:** https://orcid.org/0000-0002-1602-2330 Content not peer-reviewed by ChemRxiv. **License:** CC BY-NC-ND 4.0

2. B. S. Basavarajappa, Neuropharmacology of the endocannabinoid signaling system-molecular mechanisms, biological actions and synaptic plasticity, *Curr. Neuropharmacol.*, 2007, **5**, 81.
3. M. Maccarrone, V. D. Marzo, J. Gertsch, U. Grether, A. C. Howlett, T. Hua, A. Makriyannis, D. Piomelli, N. Ueda and M. v. d. Stelt, Goods and Bads of the Endocannabinoid System as a Therapeutic Target: Lessons Learned after 30 Years, *Pharmacol. Rev.*, 2023, **75**, 885.
4. H.-C. Lu and K. Mackie, Review of the Endocannabinoid System, *Biol. Psychiatry. Cogn. Neurosci. Neuroimaging.* , 2021, **6**, 607.
5. A. C. Howlett and M. E. Abood, in *Adv. Pharmacol.*, eds. D. Kendall and S. P. H. Alexander, Academic Press, 2017, vol. 80, p. 169.
6. R. G. Pertwee, Pharmacology of cannabinoid CB1 and CB2 receptors, *Pharmacol. Ther.*, 1997, **74**, 129.
7. E. Moreno, M. Cavic, A. Krivokuca, V. Casadó and E. Canela, The Endocannabinoid System as a Target in Cancer Diseases: Are We There Yet?, *Front. Pharmacol.*, 2019, **10**, 339.
8. A. Capozzi, V. Mattei, S. Martellucci, V. Manganelli, G. Saccomanni, T. Garofalo, M. Sorice, C. Manera and R. Misasi, Anti-Proliferative Properties and Proapoptotic Function of New CB2 Selective Cannabinoid Receptor Agonist in Jurkat Leukemia Cells, *Int. J. Mol. Sci.*, 2018, **19**, 1958.
9. M. S. García-Gutiérrez and J. Manzanares, Overexpression of CB2 cannabinoid receptors decreased vulnerability to anxiety and impaired anxiolytic action of alprazolam in mice, *J. Psychopharmacol.* , 2010, **25**, 111.
10. P. L. McGeer and E. McGeer, Conquering Alzheimer's Disease by Self Treatment, *J. Alzheimer's Dis.*, 2018, **64**, S361.
11. T. Cassano, S. Calcagnini, L. Pace, F. De Marco, A. Romano and S. Gaetani, Cannabinoid Receptor 2 Signaling in Neurodegenerative Disorders: From Pathogenesis to a Promising Therapeutic Target, *Front. Neurosci.*, 2017, **11**, 30.
12. Z. X. Xi, X. Q. Peng, X. Li, R. Song, H. Y. Zhang, Q. R. Liu, H. J. Yang, G. H. Bi, J. Li and E. L. Gardner, Brain cannabinoid CB_2 receptors modulate cocaine's actions in mice, *Nat. Neurosci.*, 2011, **14**, 1160.
13. J. Fernández-Ruiz, J. Romero, G. Velasco, R. M. Tolón, J. A. Ramos and M. Guzmán, Cannabinoid CB2 receptor: a new target for controlling neural cell survival?, *Trends Pharmacol. Sci.*, 2007, **28**, 39.
14. P. Morales, L. Hernandez-Folgado, P. Goya and N. Jagerovic, Cannabinoid receptor 2 (CB2) agonists and antagonists: a patent update, *Expert Opin. Ther. Pat.*, 2016, **26**, 843.
15. W. Bu, H. Ren, Y. Deng, N. Del Mar, N. M. Guley, B. M. Moore, M. G. Honig and A. Reiner, Mild Traumatic Brain Injury Produces Neuron Loss That Can Be Rescued by Modulating Microglial Activation Using a CB2 Receptor Inverse Agonist, *Front. Neurosci.*, 2016, **10**, 1.
16. B. Bie, J. Wu, J. F. Foss and M. Naguib, An overview of the cannabinoid type 2 receptor system and its therapeutic potential, *Curr. Opin. Anaesthesiol.*, 2018, **31**, 407.

https://doi.org/10.26434/chemrxiv-2024-q741f **ORCID:** https://orcid.org/0000-0002-1602-2330 Content not peer-reviewed by ChemRxiv. **License:** CC BY-NC-ND 4.0

17. G. C. Brailoiu, E. Deliu, J. Marcu, N. E. Hoffman, L. Console-Bram, P. Zhao, M. Madesh, M. E. Abood and E. Brailoiu, Differential Activation of Intracellular versus Plasmalemmal CB2 Cannabinoid Receptors, *Biochemistry*, 2014, **53**, 4990.

18. F. S. den Boon, P. Chameau, Q. Schaafsma-Zhao, W. van Aken, M. Bari, S. Oddi, C. G. Kruse, M. Maccarrone, W. J. Wadman and T. R. Werkman, Excitability of prefrontal cortical pyramidal neurons is modulated by activation of intracellular type-2 cannabinoid receptors, *Proc Natl Acad Sci U S A*, 2012, **109**, 3534.

19. J. T. Castaneda, A. Harui and M. D. Roth, Regulation of Cell Surface CB(2) Receptor during Human B Cell Activation and Differentiation, *J Neuroimmune Pharmacol*, 2017, **12**, 544.

20. T. Gazzi, B. Brennecke, K. Atz, C. Korn, D. Sykes, G. Forn-Cuni, P. Pfaff, R. C. Sarott, M. V. Westphal, Y. Mostinski, L. Mach, M. Wasinska-Kalwa, M. Weise, B. L. Hoare, T. Miljuš, M. Mexi, N. Roth, E. J. Koers, W. Guba, A. Alker, A. C. Rufer, E. A. Kusznir, S. Huber, C. Raposo, E. A. Zirwes, A. Osterwald, A. Pavlovic, S. Moes, J. Beck, M. Nettekoven, I. Benito-Cuesta, T. Grande, F. Drawnel, G. Widmer, D. Holzer, T. van der Wel, H. Mandhair, M. Honer, J. Fingerle, J. Scheffel, J. Broichhagen, K. Gawrisch, J. Romero, C. J. Hillard, Z. V. Varga, M. van der Stelt, P. Pacher, J. Gertsch, C. Ullmer, P. J. McCormick, S. Oddi, H. P. Spaink, M. Maccarrone, D. B. Veprintsev, E. M. Carreira, U. Grether and M. Nazaré, Detection of cannabinoid receptor type 2 in native cells and zebrafish with a highly potent, cell-permeable fluorescent probe, *Chem. Sci.*, 2022, **13**, 5539.

21. R. C. Sarott, M. V. Westphal, P. Pfaff, C. Korn, D. A. Sykes, T. Gazzi, B. Brennecke, K. Atz, M. Weise, Y. Mostinski, P. Hompluem, E. Koers, T. Miljuš, N. J. Roth, H. Asmelash, M. C. Vong, J. Piovesan, W. Guba, A. C. Rufer, E. A. Kusznir, S. Huber, C. Raposo, E. A. Zirwes, A. Osterwald, A. Pavlovic, S. Moes, J. Beck, I. Benito-Cuesta, T. Grande, S. Ruiz de Martín Esteban, A. Yeliseev, F. Drawnel, G. Widmer, D. Holzer, T. van der Wel, H. Mandhair, C.-Y. Yuan, W. R. Drobyski, Y. Saroz, N. Grimsey, M. Honer, J. Fingerle, K. Gawrisch, J. Romero, C. J. Hillard, Z. V. Varga, M. van der Stelt, P. Pacher, J. Gertsch, P. J. McCormick, C. Ullmer, S. Oddi, M. Maccarrone, D. B. Veprintsev, M. Nazaré, U. Grether and E. M. Carreira, Development of High-Specificity Fluorescent Probes to Enable Cannabinoid Type 2 Receptor Studies in Living Cells, *J. Am. Chem. Soc.*, 2020, **142**, 16953.

22. F. Spinelli, R. Giampietro, A. Stefanachi, C. Riganti, J. Kopecka, F. S. Abatematteo, F. Leonetti, N. A. Colabufo, G. F. Mangiatordi, O. Nicolotti, M. G. Perrone, J. Brea, M. I. Loza, V. Infantino, C. Abate and M. Contino, Design and synthesis of fluorescent ligands for the detection of cannabinoid type 2 receptor (CB2R), *Eur. J. Med. Chem.*, 2020, **188**, 112037.

23. S. Singh, C. R. M. Oyagawa, C. Macdonald, N. L. Grimsey, M. Glass and A. J. Vernall, Chromenopyrazole-based High Affinity, Selective Fluorescent Ligands for Cannabinoid Type 2 Receptor, *ACS Med. Chem. Lett.*, 2019, **10**, 209.

https://doi.org/10.26434/chemrxiv-2024-q741f **ORCID:** https://orcid.org/0000-0002-1602-2330 Content not peer-reviewed by ChemRxiv. **License:** CC BY-NC-ND 4.0

24. M. Sexton, G. Woodruff, E. A. Horne, Y. H. Lin, G. G. Muccioli, M. Bai, E. Stern, D. J. Bornhop and N. Stella, NIR-mbc94, a fluorescent ligand that binds to endogenous CB(2) receptors and is amenable to high-throughput screening, *Chem Biol.*, 2011, **18**, 563.

25. L. Scipioni, D. Tortolani, F. Ciaramellano, F. Fanti, T. Gazzi, M. Sergi, M. Nazaré, S. Oddi and M. Maccarrone, Aβ Chronic Exposure Promotes an Activation State of Microglia through Endocannabinoid Signalling Imbalance, *Int. J. Mol. Sci.*, 2023, **24**, 1.

26. A. Haider, J. Kretz, L. Gobbi, H. Ahmed, K. Atz, M. Bürkler, C. Bartelmus, J. Fingerle, W. Guba, C. Ullmer, M. Honer, I. Knuesel, M. Weber, A. Brink, A. M. Herde, C. Keller, R. Schibli, L. Mu, U. Grether and S. M. Ametamey, Structure–Activity Relationship Studies of Pyridine-Based Ligands and Identification of a Fluorinated Derivative for Positron Emission Tomography Imaging of Cannabinoid Type 2 Receptors, *J. Med. Chem.*, 2019, **62**, 11165.

27. WO2020002270 A1.

28. X. Li, H. Chang, J. Bouma, L. V. de Paus, P. Mukhopadhyay, J. Paloczi, M. Mustafa, C. van der Horst, S. S. Kumar, L. Wu, Y. Yu, R. van den Berg, A. P. A. Janssen, A. Lichtman, Z. J. Liu, P. Pacher, M. van der Stelt, L. H. Heitman and T. Hua, Structural basis of selective cannabinoid CB(2) receptor activation, *Nat. Commun.*, 2023, **14**, 1447.

29. R. Slavik, U. Grether, A. Müller Herde, L. Gobbi, J. Fingerle, C. Ullmer, S. D. Krämer, R. Schibli, L. Mu and S. M. Ametamey, Discovery of a High Affinity and Selective Pyridine Analog as a Potential Positron Emission Tomography Imaging Agent for Cannabinoid Type 2 Receptor, *J. Med. Chem.*, 2015, **58**, 4266.

30. A. Haider, L. Gobbi, J. Kretz, C. Ullmer, A. Brink, M. Honer, T. J. Woltering, D. Muri, H. Iding, M. Bürkler, M. Binder, C. Bartelmus, I. Knuesel, P. Pacher, A. M. Herde, F. Spinelli, H. Ahmed, K. Atz, C. Keller, M. Weber, R. Schibli, L. Mu, U. Grether and S. M. Ametamey, Identification and Preclinical Development of a 2,5,6-Trisubstituted Fluorinated Pyridine Derivative as a Radioligand for the Positron Emission Tomography Imaging of Cannabinoid Type 2 Receptors, *J. Med. Chem.*, 2020, **63**, 10287.

31. M. Guberman, M. Kosar, A. Omran, E. M. Carreira, M. Nazaré and U. Grether, Reverse-Design toward Optimized Labeled Chemical Probes – Examples from the Endocannabinoid System, *CHIMIA*, 2022, **76**, 425.

32. G. Kim, S. J. Weiss and R. L. Levine, Methionine oxidation and reduction in proteins, *Biochim. Biophys. Acta, Gen. Subj.*, 2014, **1840**, 901.

33. S. Bendels, C. Bissantz, B. Fasching, G. Gerebtzoff, W. Guba, M. Kansy, J. Migeon, S. Mohr, J.-U. Peters, F. Tillier, R. Wyler, C. Lerner, C. Kramer, H. Richter and S. Roberts, Safety screening in early drug discovery: An optimized assay panel, *J. Pharmacol. Toxicol. Methods*, 2019, **99**, 106609.

https://doi.org/10.26434/chemrxiv-2024-q741f **ORCID:** https://orcid.org/0000-0002-1602-2330 Content not peer-reviewed by ChemRxiv. **License:** CC BY-NC-ND 4.0

34. M. Honer, L. Gobbi, L. Martarello and R. A. Comley, Radioligand development for molecular imaging of the central nervous system with positron emission tomography, *Drug Discovery Today*, 2014, **19**, 1936.

35. F. Broccatelli, R. Trager, M. Reutlinger, G. Karypis and M. Li, Benchmarking Accuracy and Generalizability of Four Graph Neural Networks Using Large In Vitro ADME Datasets from Different Chemical Spaces, *Mol. Inf.*, 2022, **41**, 2100321.

36. J. W. Huffman, J. Liddle, S. Yu, M. M. Aung, M. E. Abood, J. L. Wiley and B. R. Martin, 3-(1',1'-Dimethylbutyl)-1-deoxy-Δ8-THC and related compounds: synthesis of selective ligands for the CB2 receptor, *Bioorg. Med. Chem.*, 1999, **7**, 2905.

37. N. Ouali Alami, C. Schurr, F. Olde Heuvel, L. Tang, Q. Li, A. Tasdogan, A. Kimbara, M. Nettekoven, G. Ottaviani, C. Raposo, S. Röver, M. Rogers-Evans, B. Rothenhäusler, C. Ullmer, J. Fingerle, U. Grether, I. Knuesel, T. M. Boeckers, A. Ludolph, T. Wirth, F. Roselli and B. Baumann, NF-κB activation in astrocytes drives a stage-specific beneficial neuroimmunological response in ALS, *The EMBO Journal*, 2018, **37**, e98697.

38. R. F. Porter, A. M. Szczesniak, J. T. Toguri, S. Gebremeskel, B. Johnston, C. Lehmann, J. Fingerle, B. Rothenhäusler, C. Perret, M. Rogers-Evans, A. Kimbara, M. Nettekoven, W. Guba, U. Grether, C. Ullmer and M. E. M. Kelly, Selective Cannabinoid 2 Receptor Agonists as Potential Therapeutic Drugs for the Treatment of Endotoxin-Induced Uveitis, *Molecules*, 2019, **24**, 1.

39. X. Li, T. Hua, K. Vemuri, J.-H. Ho, Y. Wu, L. Wu, P. Popov, O. Benchama, N. Zvonok, K. a. Locke, L. Qu, G. W. Han, M. R. Iyer, R. Cinar, N. J. Coffey, J. Wang, M. Wu, V. Katritch, S. Zhao, G. Kunos, L. M. Bohn, A. Makriyannis, R. C. Stevens and Z.-J. Liu, Crystal Structure of the Human Cannabinoid Receptor CB2, *Cell*, 2019, **176**, 459.

40. C. Xing, Y. Zhuang, T.-H. Xu, Z. Feng, X. E. Zhou, M. Chen, L. Wang, X. Meng, Y. Xue, J. Wang, H. Liu, T. F. McGuire, G. Zhao, K. Melcher, C. Zhang, H. E. Xu and X.-Q. Xie, Cryo-EM Structure of the Human Cannabinoid Receptor CB2-Gi Signaling Complex, *Cell*, 2020, **180**, 645.

https://doi.org/10.26434/chemrxiv-2024-q741f **ORCID:** https://orcid.org/0000-0002-1602-2330 Content not peer-reviewed by ChemRxiv. **License:** CC BY-NC-ND 4.0